PROCEEDINGS OF SCIENCE

Curvature of the QCD chiral pseudocritical line from analytic continuation

Claudio Bonati, Massimo D'Elia, Marco Mariti,Michele Mesiti*, Francesco Negro
Dipartimento di Fisica, Università di Pisa and INFN, Sezione di Pisa, Pisa, Italy
E-mail: bonati@df.unipi.it,delia@df.unipi.it,
mariti@df.unipi.it,mesiti@pi.infn.it,fnegro@pi.infn.it

Francesco Sanfilippo
School of Physics and Astronomy, University of Southampton, Southampton, United Kingdom
E-mail: bonati@df.unipi.it

We present our latest results on the determination of the curvature of the pseudo-critical line of the QCD phase diagram at the physical point, using the method of analytic continuation from an imaginary chemical potential. We also assess the impact of including a non-zero strange quark chemical potential. Our results are obtained with stout improved staggered fermions and the tree level Symanzik improved gauge action.

The 33rd International Symposium on Lattice Field Theory
14 -18 July 2015
Kobe International Conference Center, Kobe, Japan

*Speaker.

PoS(LATTICE 2015)144

1. The critical line of QCD and the method of analytic continuation

The study of the behaviour of strongly interacting matter in extreme conditions is of the utmost interest for several reasons, the physics of compact stars and the early universe being examples of natural situations where it plays a crucial role. On the experimental side, heavy ion experiments can be used to probe the phase diagram of QCD. Unfortunately, very little is known from the theoretical point of view about the QCD phase diagram at nonzero baryon density, because at present (due to the infamous *sign problem*) there are no reliable tools to make predictions from first principles about those conditions. On the other hand, at zero density and finite temperature lattice simulations have reliably confirmed the existence of a smooth crossover between a confined phase, where chiral symmetry is broken, and a deconfined phase where chiral symmetry is restored. It is then possible to define a pseudo-critical temperature[1] T_c, which identifies the position of the crossover.

It is reasonable to expect that, for small values of the baryon chemical potential μ_B, this picture still holds: we can thus define the *critical line* of QCD as the region in the phase diagram for which $T = T_c(\mu_B)$. For small values of μ_B it has also been possible to study $T_c(\mu_B)$ at the physical point with two main methods to circumvent the sign problem, namely the *Taylor expansion* approach[1, 2, 3] and *analytic continuation from an imaginary chemical potential* [4], which was recently employed in [5, 6] and in the work presented here [7]. Given the invariance of QCD under charge conjugation and expecting analyticity in μ_B, the behaviour of T_c with μ_B should be of the form

$$\frac{T_c(\mu_B)}{T_c} = 1 - \kappa \left(\frac{\mu_B}{T_c(\mu_B)} \right)^2 + O(\mu_{B,I}^4) = 1 + \kappa \left(\frac{\mu_{B,I}}{T_c(\mu_{B,I})} \right)^2 + O(\mu_{B,I}^4) \, , \tag{1.1}$$

where, in the last part of the equation, the imaginary baryon chemical potential $\mu_{B,I} = -i\mu_B$ has been introduced. The main goal of the present work is to determine the coefficient κ, the curvature of the pseudocritical (or crossover) line of QCD, performing a thorough analysis of the systematics involved to obtain a reliable continuum extrapolated value.
We mainly run simulations at zero strange quark chemical potential, $\mu_s = 0$. In the aim of comparing our results with the ones coming from heavy ion collision experiments (where the strangeness S is zero), this is not a priori the right setup: the interactions give nonzero cross susceptibilities $\partial n_s / \partial \mu_l$, and in order to achieve *strangeness neutrality* we should fine-tune the values of μ_l and μ_s to have $S = 0$ (e.g. at $T = T_c$ the strangeness neutrality condition would require $\mu_s \simeq 0.25\mu_l$ [8]). In view of this, we decided to check what is the effect of a nonzero μ_s in a range which covers the strangeness neutrality condition, studying also the setup $\mu_s = \mu_l$.

2. Observables

For the determination of the critical temperature as a function of the chemical potential, we used 3 different prescriptions based on 3 different chiral observables, namely the chiral condensate renormalized in two different ways (introduced in [9] and [3], respectively) and the full renormal-

[1] The definition has a certain level of arbitrarity, as it will be clarified in the next section.

ized chiral susceptibility [10], defined as follows:

$$\langle\bar{\psi}\psi\rangle^r_{(1)}(T) \equiv \frac{\langle\bar{\psi}\psi\rangle_{ud}(T) - \frac{2m_{ud}}{m_s}\langle\bar{s}s\rangle(T)}{\langle\bar{\psi}\psi\rangle_{ud}(0) - \frac{2m_{ud}}{m_s}\langle\bar{s}s\rangle(0)} \tag{2.1}$$

$$\langle\bar{\psi}\psi\rangle^r_{(2)}(T) \equiv \frac{m_{ud}}{m_\pi^4}\left(\langle\bar{\psi}\psi\rangle_{ud} - \langle\bar{\psi}\psi\rangle_{ud}(0)\right) \tag{2.2}$$

$$\chi^r_{\bar{\psi}\psi}(T) \equiv \frac{m_{ud}^2}{m_\pi^4}\left[\chi_{\bar{\psi}\psi}(T) - \chi_{\bar{\psi}\psi}(0)\right] . \tag{2.3}$$

We take the crossover temperature at the inflection point for the condensates, and at the maximum in the case of the chiral susceptibility, locating these points by a fitting procedure (see Fig.1). The data for the renormalized chiral condensate(s) has been fitted with the function

$$\langle\bar{\psi}\psi\rangle^r(T) = A_1 + B_1 \arctan\left[C_1\left(T - T_c\right)\right] , \tag{2.4}$$

while for the renormalized chiral susceptibility we opted for a Lorentzian form:

$$\chi^r_{\bar{\psi}\psi}(T) = \frac{A_2}{(T-T_c)^2 + B_2^2} . \tag{2.5}$$

These prescriptions to locate the pseudocritical temperature are *faithful*, in the sense that in the case of a real phase transition they would yield the corresponding critical temperature. The procedure we have followed is to determine T_c for a number of values of $\mu_{B,I}$ and fit the data points with the expression in Eq.(1.1) to obtain κ.

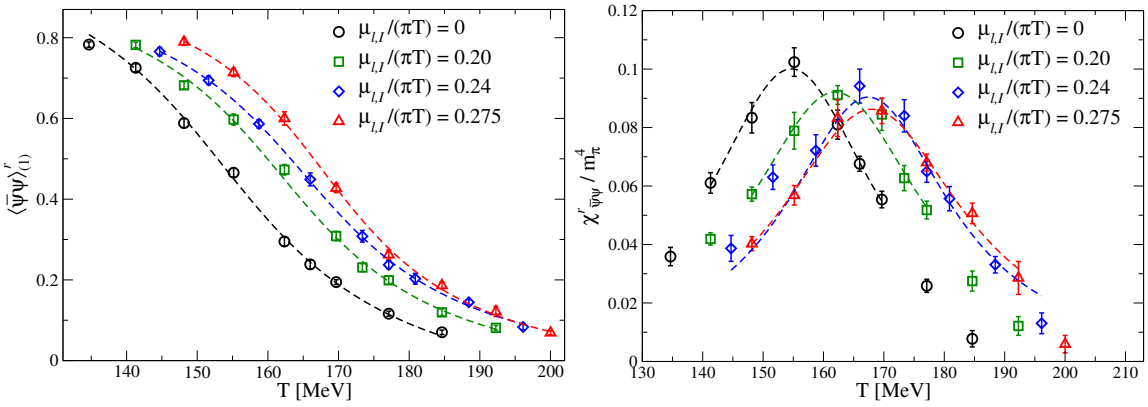

Figure 1: Dependence of the renormalized observables on the temperature. The result of the fit with the functions (2.4) and (2.5) is also plotted. (from [7]). **Left:** renormalized chiral condensate $\langle\bar{\psi}\psi\rangle^r_{(1)}$. **Right:** renormalized chiral susceptibility $\chi^r_{\bar{\psi}\psi}$.

3. Numerical setup

We simulated the theory on the lattice using a tree level Symanzik improved gauge action and a root-staggered stout improvement for the fermion part of the action, *at the physical point*. In order to do this, we tuned the quark masses as a function of β following the *line of constant physics*

obtained in [11] (see [7] for details).

For finite size effects, we refer to the analysis already done in a previous study [7]. In that work, using data coming from $N_t = 6$ lattices, we have shown that finite size effects are negligible on lattices having aspect ratio ≥ 4. For this reason, we have since then run simulations on $32^3 \times 8$, $40^3 \times 10$ and $48^3 \times 12$ lattices in order to perform a continuum limit extrapolation of κ in the setup $\mu_s = 0$. To calculate renormalized observables we also had to measure bare quantities at zero temperature. This was performed on 32^4 and 48^4 lattices for sparse values of β, and the full dependence of the bare zero-temperature observables on the coupling was obtained through a suitable interpolation. Moreover, in order to investigate the effect of a nonzero μ_s, on the $32^3 \times 8$ lattice we have studied the setup $\mu_s = \mu_l$ and $\mu_s = 0$, for several values of μ_l.

4. Numerical results

In order to check the systematics involved in the continuum limit we performed this in two ways, namely on the curvature κ directly or on the observables. The second procedure yields continuum extrapolated values of $T_c(\mu_B)$, which are fitted giving a second estimate of the curvature in the continuum limit.

A little remark about uncertainties is in order. The procedure explained in section 2 to locate the critical temperature requires a fit whose result is dependent both on the choice of the fit range and on the form of the function used. We assessed the systematic errors on $T_c(\mu_B)$ by varying the fit range and changing the function used in the fit to a similar one, while the statistical uncertainties were estimated making use of a boostrap analysis.

4.1 The effect of a nonzero μ_s

In Fig. 2 we show our results about the effect of a nonzero μ_s. The same figure shows also the results for κ that one can obtain trying different fitting strategies, that is varying the form (quadratic or quartic in μ_I), and varying the upper limit of the fit range.

The result of this analysis is that, up to the present level of accuracy, the values of κ obtained in the $\mu_s = 0$ and $\mu_s = \mu_l$ cases are compatible if a quartic term in $\mu_{l,I}$ is taken into consideration on the latter situation. In fact, omitting that term and fitting the data for $\mu_s = \mu_l$ just with a quadratic expression, the obtained χ^2/n_{dof} is 2.4, while including that term $\chi^2/n_{dof} \leqslant 1$. If we restrict ourselves to a quadratic expression, we see that in the case $\mu_s = \mu_l$ the result for κ is not stable with the fit range: if we reduce the fit range to small values of μ we obtain, again, compatible values for the curvature from the $\mu_s = \mu_l$ and the $\mu_s = 0$ cases. For this reason, we don't expect the curvature measured in the strangeness neutrality condition to be significantly different from the value obtained in our work.

4.2 The continuum limit

With the first procedure we calculated a value of the curvature for each value of N_t (6,8,10 and 12) and extrapolated to the continuum limit assuming corrections of order $1/N_t^2$. We obtained $\kappa = 0.0134(13), 0.0127(14), 0.0132(10)$ from the renormalized chiral condensate I, II and

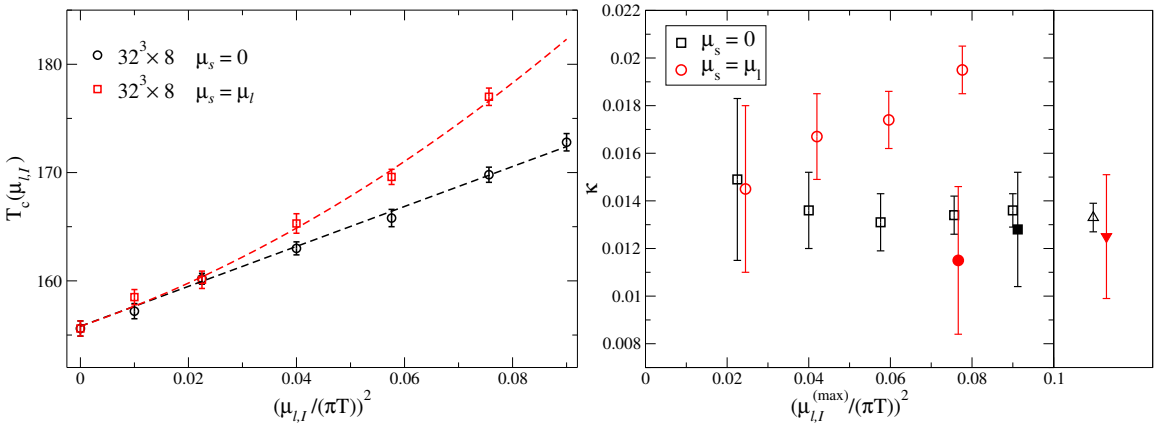

Figure 2: The effect of the inclusion of a nonzero chemical potential. **Left:** the critical line in the two cases, $\mu_s = 0$ (red) and $\mu_s = \mu_l$ (black). **Right:** analysis of the dependence of the estimate of the curvature κ on the upper fit range limit $\mu_{l,I}^{(max)}$ (see explanation in the main text). Black data points refer to the $\mu_s = 0$ setup while Red data points refer to the $\mu_s = \mu_l$ case. Filled symbols refer to quartic fits in $\mu_{l,I}$ while empty symbols show the results for quadratic fits in $\mu_{l,I}$. The data points on the right are the result of a combined fit (quartic for the $\mu_s = \mu_l$ case, and quadratic for $\mu_s = 0$) on all data points available.

the renormalized chiral susceptibility respectively; this procedure is shown in Fig. 5.

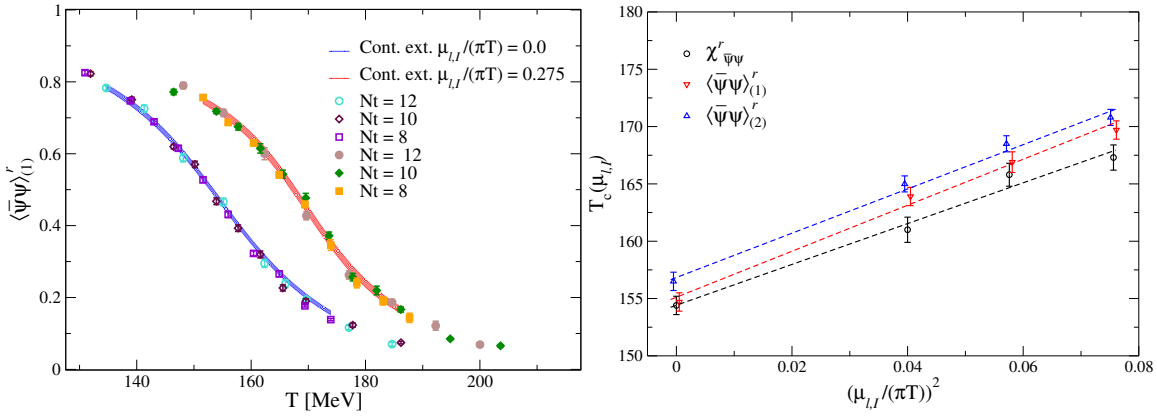

Figure 3: Continuum limit of the observables. **Left:** renormalized chiral condensate (Eq. 2.1). **Right :** critical lines in the $\mu_{l,I}$ versus T plane obtained with the method of continuum extrapolated observables.

With the second procedure, instead, we assumed a dependence of the observables of the kind shown in Eqs. (2.4) and (2.5), where all or part of the coefficient are assumed to have a dependence on the lattice spacing in the form $const + a/N_t^2$ [2]. By making use of data from $N_t = 8$,10 and 12 lattices we obtained the continuum extrapolated values of the observables as a function of T, as shown in Figs. 3 and 4, as well as a continuum extrapolated estimate of T_c. We then fitted the $T_c(\mu)$ with the form of Eq.(1.1) and obtained $\kappa = 0.0145(11), 0.0138(10), 0.0131(12)$ from

[2] More precisely, we assumed such dependence for all the coefficients in Eq.(2.5) for the chiral susceptibility, while for the chiral condensates such dependence was assumed only on the T_c and C_1 parameters in Eq.(2.4).

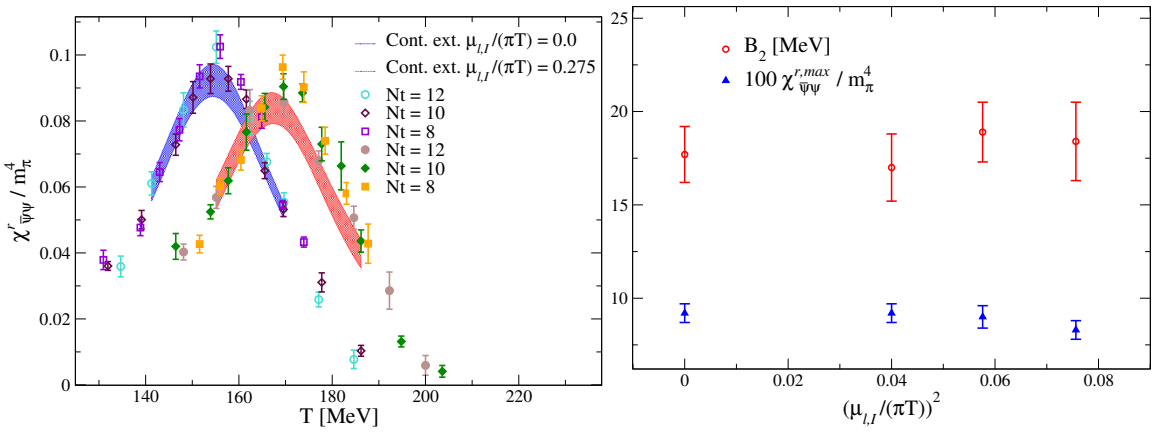

Figure 4: Continuum limit of the observables, from the renormalized chiral susceptibility (Eq. 2.3). **Left:** renormalized chiral susceptibility as a function of T. **Righ:** behaviour of the height $\chi^{r,max}_{\bar\psi\psi}$ and the width B_2 of the peak of the susceptibility as a function of the chemical potential.

$\langle\bar\psi\psi\rangle^r_{(1)}$, $\langle\bar\psi\psi\rangle^r_{(2)}$, and $\chi^r_{\bar\psi\psi}$ respectively: this procedure is shown in Fig. 3, and we notice that these results are compatible with the ones obtained with the first method.

As a byproduct of this second procedure, we got also continuum limit estimates of the witdh and the height of the peak of the susceptibility as a function of the imaginary chemical potential, which are shown in Fig. 4. In the spirit of analytic continuation, this information could give hints for or against a critical point for real chemical potential. While our data don't show any influence of a possible endpoint nearby, it must be said that the Roberge-Weiss endpoint (which, in the setup with $\mu_s = 0$, lies at $\mu_{l,I}/(\pi T) \sim 0.45$ [7]) seems not to have any influence on these quantities either.

As a conclusion of our work, considering also the uncertainty derived from the strangeness neutrality issue, we give $\kappa = 0.0135(20)$ as a prudential estimate of the curvature of the chiral crossover line. In Fig. 5 we show the comparison of our value with the ones obtained in the recent literature at the physical point. While it appears that that there is "tension" between the results with the Taylor expansion method (the upper 4 points in the plot) and the ones obtained with analytic continuation (the others), it must be noted that the discrepancy is significantly reduced if one considers only the most recent results.

References

[1] S. Borsanyi, G. Endrodi, Z. Fodor, S. D. Katz, S. Krieg, C. Ratti and K. K. Szabo, JHEP **1208**, 053 (2012) [arXiv:1204.6710 [hep-lat]]. O. Kaczmarek, F. Karsch, E. Laermann, C. Miao, S. Mukherjee, P. Petreczky, C. Schmidt, W. Soeldner and W. Unger, Phys. Rev. D **83**, 014504 (2011) [arXiv:1011.3130 [hep-lat]].

[2] P. Hegde *et al.* [Bielefeld-BNL-CCNU Collaboration], arXiv:1511.03378 [hep-lat].

[3] G. Endrodi, Z. Fodor, S. D. Katz and K. K. Szabo, JHEP **1104**, 001 (2011) [arXiv:1102.1356 [hep-lat]].

[4] P. de Forcrand and O. Philipsen, Nucl. Phys. B **642**, 290 (2002) [hep-lat/0205016]; Nucl. Phys. B **673**, 170 (2003) [hep-lat/0307020]. M. D'Elia and M. P. Lombardo, Phys. Rev. D **67**, 014505 (2003)

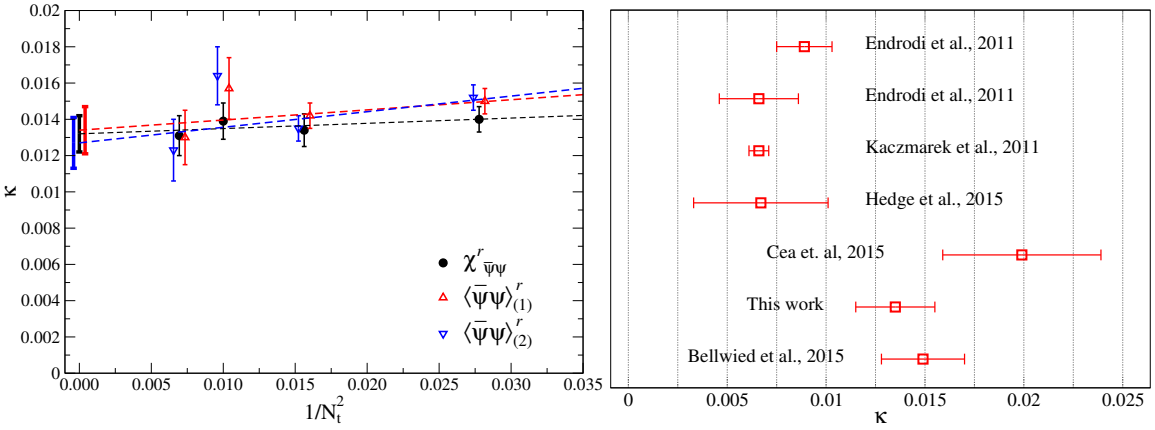

Figure 5: Estimate of the curvature of the pseudocritical line. **Left:** our continuum extrapolated result (first method) for κ. **Right:** values of κ from the literature.

[hep-lat/0209146]; Phys. Rev. D **70**, 074509 (2004) [hep-lat/0406012]. V. Azcoiti, G. Di Carlo, A. Galante and V. Laliena, Nucl. Phys. B **723**, 77 (2005) [hep-lat/0503010]. L. K. Wu, X. Q. Luo and H. S. Chen, Phys. Rev. D **76**, 034505 (2007) [hep-lat/0611035]. P. Cea, L. Cosmai, M. D'Elia and A. Papa, Phys. Rev. D **77**, 051501 (2008) [arXiv:0712.3755 [hep-lat]]. K. Nagata and A. Nakamura, Phys. Rev. D **83**, 114507 (2011) [arXiv:1104.2142 [hep-lat]]. P. Cea, L. Cosmai, M. D'Elia, A. Papa and F. Sanfilippo, Phys. Rev. D **85**, 094512 (2012) [arXiv:1202.5700 [hep-lat]]. E. Laermann, F. Meyer and M. P. Lombardo, J. Phys. Conf. Ser. **432**, 012016 (2013).

[5] P. Cea, L. Cosmai and A. Papa, Phys. Rev. D **89**, 074512 (2014) [arXiv:1403.0821 [hep-lat]]. Phys. Rev. D **93**, 014507 (2016) [arXiv:1508.07599 [hep-lat]].

[6] R. Bellwied, S. Borsanyi, Z. Fodor, J. Günther, S. D. Katz, C. Ratti and K. K. Szabo, Phys. Lett. B **751**, 559 (2015) [arXiv:1507.07510 [hep-lat]].

[7] C. Bonati, M. D'Elia, M. Mariti, M. Mesiti, F. Negro and F. Sanfilippo, Phys. Rev. D **90**, 114025 (2014) [arXiv:1410.5758 [hep-lat]]. Phys. Rev. D **92**, 054503 (2015) [arXiv:1507.03571 [hep-lat]].

[8] A. Bazavov *et al.*, Phys. Rev. Lett. **113**, 072001 (2014) [arXiv:1404.6511 [hep-lat]]. S. Borsanyi, Z. Fodor, S. D. Katz, S. Krieg, C. Ratti and K. K. Szabo, Phys. Rev. Lett. **111**, 062005 (2013) [arXiv:1305.5161 [hep-lat]].

[9] M. Cheng, N. H. Christ, S. Datta, J. van der Heide, C. Jung, F. Karsch, O. Kaczmarek and E. Laermann *et al.*, Phys. Rev. D **77**, 014511 (2008) [arXiv:0710.0354 [hep-lat]].

[10] Y. Aoki, S. Borsanyi, S. Durr, Z. Fodor, S. D. Katz, S. Krieg and K. K. Szabo, JHEP **0906**, 088 (2009) [arXiv:0903.4155 [hep-lat]].

[11] S. Borsanyi, G. Endrodi, Z. Fodor, A. Jakovac, S. D. Katz, S. Krieg, C. Ratti and K. K. Szabo, JHEP **1011**, 077 (2010) [arXiv:1007.2580 [hep-lat]].